Observations of Early Stage Graphene Growth on Copper

K. Celebi,[a] M. T. Cole,[b] K. B. K. Teo,[c] and H. G. Park[a,*,z]

[a]*Department of Mechanical & Process Engineering, ETH Zurich, Zurich CH-8092, Switzerland*
[b]*Department of Engineering, Electrical Engineering Division, University of Cambridge, Cambridge CB3 0FA, United Kingdom*
[c]*AIXTRON Ltd, Buckingway Business Park, Swavesey, Cambridge CB24 4FQ, United Kingdom*

We present our observations made during the early stages of graphene growth employing an ethylene-based CVD method capable of synthesizing copper-foil-catalyzed monolayer graphene at temperatures as low as 800°C. Spectroscopic monitoring of surface catalysis showed that graphene crystals evolve from densely distributed nucleation points that interconnect to form large crystals covering the entire surface. Secondary nucleation was observed inside the primary graphene crystals. An effective activation energy for copper-catalyzed ethylene-based graphene synthesis was determined to be 2.46 eV, a value that suggests surface dehydrogenation of ethylene or lattice integration of graphene as the possible rate-determining step in the heterogeneous catalysis.
© 2011 The Electrochemical Society. [DOI: 10.1149/2.005201esl] All rights reserved.

Graphene, a two-dimensional atomic layer of sp^2-hybridized carbon atoms, has attracted great scientific and technological interest since its discovery in its free-standing form.[1,2] Recent demonstrations of graphene synthesis by chemical vapor deposition (CVD) on metal substrates demonstrated that CVD is perhaps one of the most scalable methods for obtaining high-quality graphene yields over large-areas.[3–5] Of these metals, copper has been repeatedly implicated as the most feasible graphene catalyst due to its low carbon solubility, low-cost, self-terminating catalysis tendencies and the ease of graphene transfer.[4,6,7] An important point in synthesizing high-quality graphene is the use of increasingly reactive carbon precursors. Currently, one widely used precursor is methane,[4,6] known to be cleaner than other conventional carbon precursors such as acetylene.[8,9] Nonetheless, high temperatures are necessary to induce its thermal decomposition compared to other precursors.[10] However, compared to acetylene and methane, ethylene has an intermediate reactivity,[9,11] which promises increased controllability and intermediate-temperature growth. The graphene quality can be further improved by tuning the hydrogen partial pressure. This suppresses the precursors decomposition rate[12] and increases the amorphous carbon etch rate.[13] Although these two hydrogen-related properties improve the quality of the graphene, they can however detrimentally transform lattice sp^2 bonds into sp^3,[14] thereby degrading the crystallographic quality of the graphene. In this sense, ethylene has a significant advantage over methane because of its large tolerance toward hydrogen concentration.[15] Earlier studies on metal-catalyzed graphene synthesis demonstrated ethylene-based growths on Ir(111),[16] Ru(0001)[17] and Cu(111);[18] however, large-scale, ethylene-based CVD of graphene on copper foils has only been reported much more recently.[19]

Here we report on our continuing efforts towards the use of ethylene as a viable precursor for graphene CVD on copper and our observations on the early stages of synthesis at moderate growth temperatures and pressures. Our study on the evolution of the domain structure over both time and temperature demonstrates continuous graphene covering at reduced temperatures (≤850°C) compared to methane-based CVD (1000°C).[4]

Experimental

All growths were carried out in a commercially available CVD reactor (AIXTRON Black Magic). For a typical process, at 3.1 Torr, (Figure 1a), copper foils (Alfa Aesar, 25 μm, 99.8%) were reduced at 850°C (measured by surface infrared pyrometry) under 20 sccm of hydrogen diluted with 1500 sccm of argon for 30 min. Monolayers were grown over 10 min *via* the addition of 7 sccm of ethylene

without altering the hydrogen and argon flows. Ethylene exposure was terminated immediately prior to cooling to prevent further pyrolysis and deposition of amorphous deposits. Monolayer graphene grew at temperatures as low as 800°C. No graphene growth was observed at temperatures less than this.

As-grown graphene samples were characterized by Raman spectroscopy, a widely used non-destructive technique that quantifies the defect density and crystallographic quality in carbonaceous products.[20] Raman measurements were performed using both 457-nm and 532-nm excitations, as illustrated in Figure 1b. Note that copper substrates induce potentially significant fluorescence backgrounds.[21] 457-nm, rather than 532-nm, laser excitation markedly reduces such backgrounds (Figure 1b). In order for more conclusive and corroborating characterizations, the films were transferred to 150-nm-thick thermal oxidized silicon substrates *via* a polymer-mediated transfer process. The copper support was back etched using 1 M ferric chloride.[4,5] These transferred films were characterized by micro-Raman spectroscopy using 532-nm excitation (2 mW) with a focal spot size of *ca.* 0.4 μm (WiTec CRM 200) and a 457-nm excitation (3 mW) with a spot size of *ca.* 1.2 μm (Renishaw inVia). The surface morphology of the as-grown graphene films directly on the copper foils was characterized by field emission scanning electron microscopy (Zeiss Gemini 1530 FEG).

Results and Discussion

Graphene grows on copper by surface catalysis initiated by a seed or nucleation site.[4,7] Crystals subsequently enlarge laterally by the addition of carbon atoms to the edges of the growing domain.[7] For low-pressure CVD, this nucleation occurs heterogeneously and typically results in the formation of four-lobed crystals, where each lobe has a distinct crystal orientation due to the dominance of the four-fold symmetry of the copper surface.[22] However, for atmospheric pressure CVD, crystals are typically hexagonal due to the dominance of the graphene's six-fold symmetry.[23] In our case, as the pressure lies between these two extremes, the domains are more circular and show a mixture of both four- and six-fold symmetries. To capture the crystal shape and partial covering at the very early stages of graphene growth, low ethylene partial pressures were employed and either the growth time (for a fixed temperature-850°C) or growth temperature (for a fixed growth time-5 min) were varied. The crystal evolution over time and temperature is summarized in the SEM micrographs of Figure 2. Rather expectedly, the graphene domain size increases nonlinearly with increasing the growth time. More interestingly, crystals also evidence enhanced growth rates for temperatures greater than 800°C (Figures 2e–2h). The temperature dependence of the growth rate suggests an effective activation energy of 2.46 eV. Further studies elaborating on the activation energy of copper-catalyzed graphene

* Electrochemical Society Active Member.
z E-mail: parkh@ethz.ch
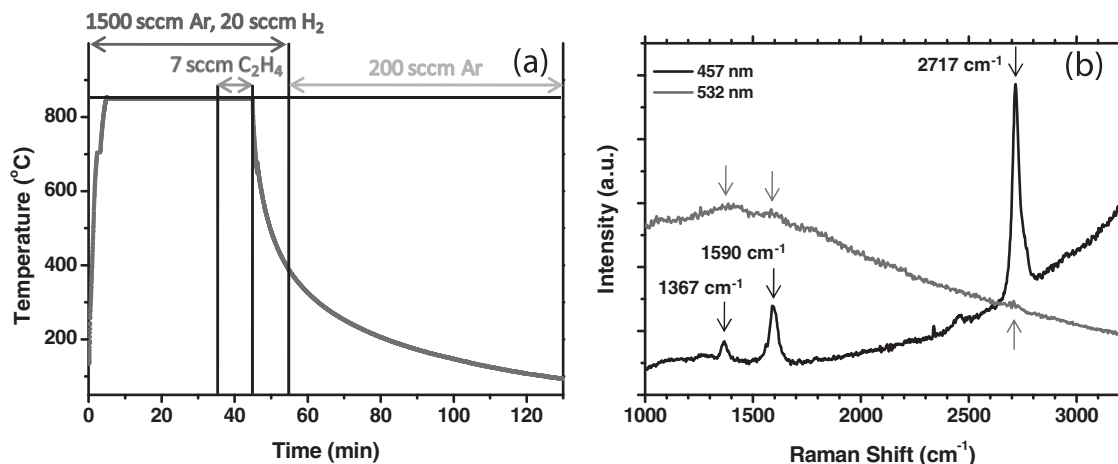
Figure 1. (a) A typical CVD growth scheme. The red curve shows the sample temperature measured by an infrared pyrometry. (b) Comparison of the Raman spectra taken on the as-grown graphene on copper foil using 457-nm (black) and 532-nm excitations (red). The arrows indicate the major Raman *D*, *G* and *G'* peaks (*from left to right*).

will be presented elsewhere. Considering the very low energies for hydrocarbon adsorption and carbon diffusion on copper (typically <0.1 eV),[15] the rate-limiting step for copper-catalyzed graphene growth is deemed to include either ethylene surface dehydrogenation or carbon lattice integration. Indeed, the estimated effective activation energy shows good agreement with the calculated dehydrogenation energy of ethylene on copper[15] and carbon lattice-integration estimates.[24] The graphene domain density decreases as the growth time increases. We speculate that this decrease is related to the amalgamation of smaller

domains. However, the spacing between the domains tends to increase with time (up until the 10 min growth), which tentatively suggests possible migration of the graphene domains during high-temperature growth.

Raman spectroscopic analysis quantitatively bolsters the SEM observations. Figure 3 shows the Raman spectra of graphene films
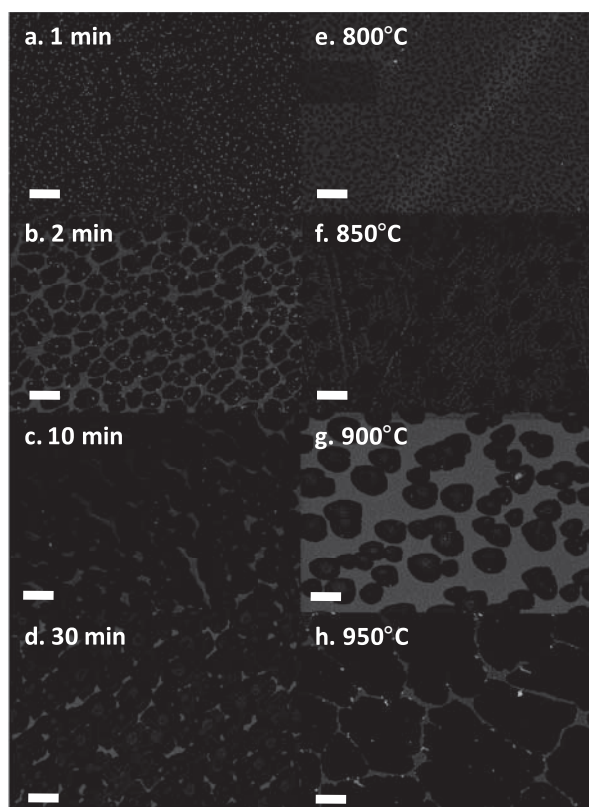
Figure 2. SEM micrographs of as-grown graphene on copper foils. Grown at 850°C for: 1 min (a), 2 min (b), 10 min (c) and 30 min (d). Grown for 5 min at: 800°C (e), 850°C (f), 900°C (g) and 950°C (h). Dark regions correspond to the graphene domains (scale bar: 2 μm).
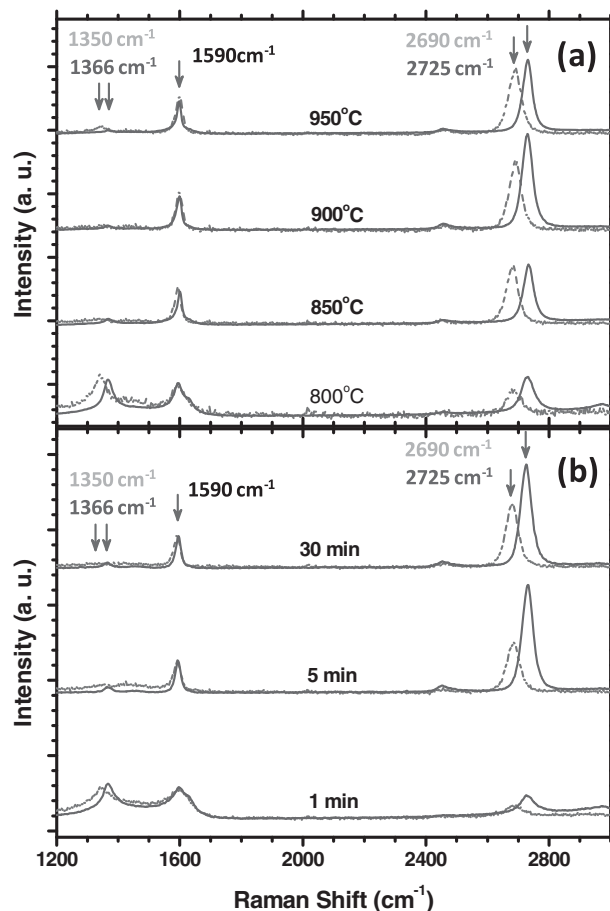
Figure 3. Raman spectra of a time series (a) and temperature series (b). Green (blue) curves show the Raman data for the 532-nm (457-nm) excitation. For the time series, the temperature was maintained at 850°C. For the temperature series the growth time was maintained at 5 min.
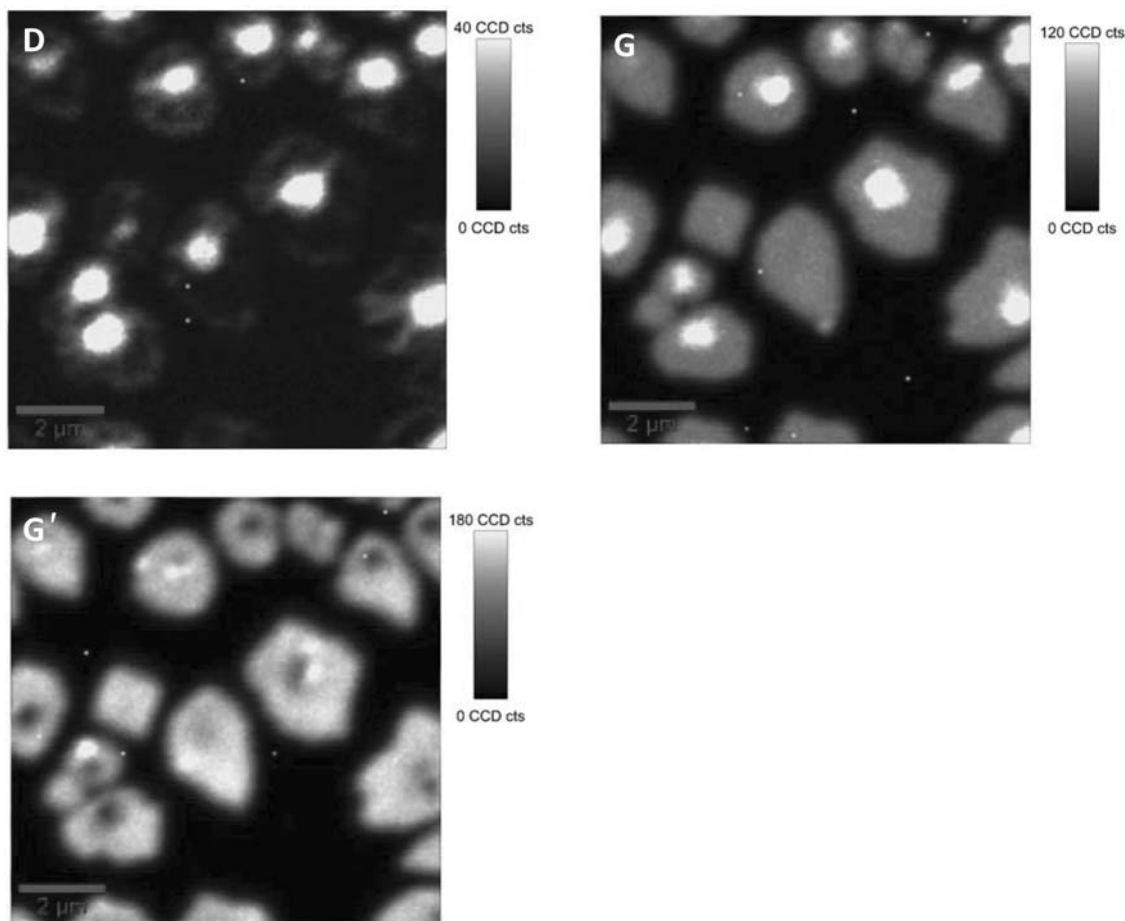
Figure 4. Micro-Raman (532 nm) spatial maps of the *D*, *G*, *G'* peaks of the transferred graphene on SiO$_2$. Note the secondary nucleation sites in the flake interiors.

(transferred to SiO$_2$) grown at different temperatures (Figure 3a) and for various durations (Figure 3b). All spectra show the three major Raman peaks: *D*, *G* and *G'*. The *G'* peak is key in determining the film thickness, since this band originates from a double resonant process involving the generation of electron-hole pairs, a splitting in the electronic bands caused by interlayer coupling in multi-layer graphene induces a deviation from the single Lorentzian behavior.[20,25] The standard interpretation here is that a single-Lorentzian-fitted *G'* peak indicates monolayer graphene.[20] Since consideration of the *G'* peak's shape alone may be somewhat misleading for thick, turbostratically ordered multilayer graphene with subsequent electronic decoupling,[26] it is important to examine the *G'* peaks position and intensity as well. Indeed, the peak position (2690 cm^{-1}) and high intensity strongly support the monolayer nature of our films.[5,20,25] The low intensity of the *D* peak also indicates a rather low defect density of the basal plane. The positions of the *D*, *G* and *G'* peaks are 1350 cm^{-1}, 1590 cm^{-1} and 2690 cm^{-1}, respectively for the 532-nm excitation and around 1366 cm^{-1}, 1590 cm^{-1} and 2725 cm^{-1} for the 457-nm. The shifts in *D* and *G'* peaks are a result of their dispersive nature.[27] The small domain samples (800°C/1 min) show highly prominent *D* peaks and three additional disorder-oriented peaks at 1450 cm^{-1}, 1620 cm^{-1} (*D'*), and 2900 cm^{-1} (*D+D'*) during 532-nm excitation. These features are attributed to incomplete crystallization and edge-state dominance at this very early stage nucleation. The consequent decrease in the *G* and *G'* peaks is caused by the small number of phonons within these nanocrystalline domains.[28]

We further characterized the domain structure by micro-Raman spatial mapping. Figure 4 shows areal scans for the three major Raman peaks of a transferred graphene sample (850°C/5 min). Black regions represent bare SiO$_2$. The edges of the primary graphene domains are distinguished by local increases in the *D* peak that originates from the edge disorder. While most of the graphene domains show monolayer spectroscopic characteristics, some domain centers exhibit clear deviations from this and the increased *D* peak indicates edge-state defects associated with secondary nucleation. This localized layer doubling caused by secondary nucleation decreases the *G'* peak, but increases the *G* peak *via* the provision of an increased phonon density. These secondary nucleations may in part be a result of total growth pressures (3.1 Torr), higher than those of methane-based CVD.[4,29] Increasing the growth pressure decreases copper sublimation allowing for the thermally-stimulated formation of copper plateaus, which initiates epitaxial growth of the secondary graphene layers around the defective nucleation centers. A similar effect was recently demonstrated for methane-based atmospheric pressure CVD.[29]

Conclusions

We have demonstrated the low-temperature (800°C) use of ethylene as a copper-catalyzed, CVD monolayer graphene precursor. We observed a decreased crystal density with respect to time, indicating possible surface migration and domain interconnection during early stage growth. Our Raman analysis evidences secondary nucleation sites around the centers of the larger graphene domains, attributed to inhibited copper sublimation – a direct result of the growth pressure. We have determined an effective activation energy for ethylene-based CVD on copper to be 2.46 eV, from which we speculate that the possible rate limiting steps could include ethylene surface dehydrogenation and graphene lattice construction.

References

1. K. S. Novoselov, A. K. Geim, S. V. Morozov, D. Jiang, Y. Zhang, S. V. Dubonos, I. V. Grigorieva, and A. A. Firsov, *Science*, **306**, 666 (2004).
2. A. K. Geim, and K. S. Novoselov, *Nat. Mater.*, **6**, 183 (2007).
3. K. S. Kim, Y. Zhao, H. Jang, S. Y. Lee, J. M. Kim, K. S. Kim, J.-H. Ahn, P. Kim, J.-Y. Choi, and B. H. Hong, *Nature*, **457**, 706 (2009).
4. X. Li, W. Cai, J. An, S. Kim, J. Nah, D. Yang, R. Piner, A. Velamakanni, I. Jung, E. Tutuc, S. K. Banerjee, L. Colombo, and R. S. Ruoff, *Science*, **324**, 1312 (2009).
5. A. Reina, X. Jia, J. Ho, D. Nezich, H. Son, V. Bulovic, M. Dresselhaus, and J. Kong, *Nano Lett.*, **9**, 30 (2009).
6. S. Bae, H. Kim, Y. Lee, X. Xu, J.-S. Park, Y. Zheng, J. Balakrishnan, T. Lei, H. Ri Kim, Y. I. Song, Y.-J. Kim, K. S. Kim, B. Ozyilmaz, J.-H. Ahn, B. H. Hong, and S. Iijima, *Nat Nano*, **5**, 574 (2010).
7. X. Li, W. Cai, L. Colombo, and R. Ruoff, *Nano Lett.*, **9**, 4268 (2009).
8. C. L. Cheung, A. Kurtz, H. Park, and C. M. Lieber, *J. Phys. Chem. B*, **106**, 2429 (2002).
9. K. Hernadi, A. Fonseca, J. B. Nagy, A. Siska, and I. Kiricsi, *Appl. Catal., A*, **199**, 245 (2000).
10. Y.-H. Lee, and J.-H. Lee, *Appl. Phys. Lett.*, **96**, 083101 (2010).
11. M. Stadermann, S. P. Sherlock, J.-B. In, F. Fornasiero, H. G. Park, A. B. Artyukhin, Y. Wang, J. J. De Yoreo, C. P. Grigoropoulos, O. Bakajin, A. A. Chernov, and A. Noy, *Nano Lett.*, **9**, 738 (2009).
12. Y.-Q. Xu, E. Flor, H. Schmidt, R. E. Smalley, and R. H. Hauge, *Appl. Phys. Lett.*, **89**, 123116 (2006).
13. A. Okita, Y. Suda, A. Oda, J. Nakamura, A. Ozeki, K. Bhattacharyya, H. Sugawara, and Y. Sakai, *Carbon*, **45**, 1518 (2007).
14. G. Zhang, D. Mann, L. Zhang, A. Javey, Y. Li, E. Yenilmez, Q. Wang, J. P. McVittie, Y. Nishi, J. Gibbons, and H. Dai, *Proc. Natl. Acad. Sci. U. S. A.*, **102**, 16141 (2005).
15. W. Zhang, P. Wu, Z. Li, and J. Yang, *arXiv:1101.3851* (2011).
16. J. Coraux, T. N'Diaye, M. Engler, C. Busse, D. Wall, N. Buckanie, F. J. M. zu Heringdorf, R. van Gaste, B. Poelsema, and T. Michely, *New J. Phys.*, **11**, 023006 (2009).
17. A. L. Vazquez de Parga, F. Calleja, B. Borca, M. C. G. Passeggi, J. J. Hinarejos, F. Guinea, and R. Miranda, *Phys. Rev. Lett.*, **100**, 056807 (2008).
18. L. Gao, J. R. Guest, and N. P. Guisinger, *Nano Lett.*, **10**, 3512 (2010).
19. H. Shu-Jen, S. Yanning, A. A. Bol, W. Haensch, and C. Zhihong, in *Symp. on VLSI Tech. (VLSIT)*, p. 231 (2010).
20. L. M. Malard, M. A. Pimenta, G. Dresselhaus, and M. S. Dresselhaus, *Phys. Rep.*, **473**, 51 (2009).
21. P. Apell, R. Monreal, and S. Lundqvist, *Phys. Scr.*, **38**, 174 (1988).
22. J. M. Wofford, S. Nie, K. F. McCarty, N. C. Bartelt, and O. D. Dubon, *Nano Lett.*, **10**, 4890 (2010).
23. A. W. Robertson, and J. H. Warner, *Nano Lett.*, **11**, 1182 (2011).
24. E. Loginova, N. C. Bartelt, P. J. Feibelman, and K. F. McCarty, *New J. Phys.*, **10**, 093026 (2008).
25. A. C. Ferrari, J. C. Meyer, V. Scardaci, C. Casiraghi, M. Lazzeri, F. Mauri, S. Piscanec, D. Jiang, K. S. Novoselov, S. Roth, and A. K. Geim, *Phys. Rev. Lett.*, **97**, 187401 (2006).
26. J. Hass, F. Varchon, J. E. Millán-Otoya, M. Sprinkle, N. Sharma, W. A. de Heer, C. Berger, P. N. First, L. Magaud, and E. H. Conrad, *Phys. Rev. Lett.*, **100**, 125504 (2008).
27. M. J. Matthews, M. A. Pimenta, G. Dresselhaus, M. S. Dresselhaus, and M. Endo, *Phys. Rev. B*, **59**, R6585 (1999).
28. C. Casiraghi, A. Hartschuh, H. Qian, S. Piscanec, C. Georgi, A. Fasoli, K. S. Novoselov, D. M. Basko, and A. C. Ferrari, *Nano Lett.*, **9**, 1433 (2009).
29. L. Fan, Z. Li, Z. Xu, K. Wang, J. Wei, X. Li, J. Zou, D. Wu, and H. Zhu, *AIP Adv.*, **1**, 032145 (2011).